UNITED NATIONS
UNIVERSITY
GEOTHERMAL TRAINING PROGRAMME
Orkustofnun, Grensásvegur 9,
IS-108 Reykjavík, Iceland

Reports 2009
Number 13

INJECTION TEST AND EARLY PRODUCTION HISTORY OF WELL THG-1 AT THEISTAREYKIR GEOTHERMAL FIELD, N-ICELAND

Kayad Moussa Ahmed
Centre d´Etude et de Recherche de Djibouti (CERD)
Route de l´Aeroport, BP. 486
Djibouti
REPUBLIC OF DJIBOUTI
Kayadahmed2000@yahoo.fr

ABSTRACT

The Theistareykir field is located in the volcanic rift zone in N-Iceland and has abundant geothermal surface manifestations. One of the wells in this area, THG-1, was vertically drilled. After completion of the well, THG-1 was tested for its pressure response to step injection. The data were analysed by using the computer programs WellTester and Lumpfit. The skin factor for the well is estimated to be around -2, the transmissivity of the surrounding formations around 2×10^{-8} m^3/Pa·s, and the formation storage about 2×10^{-8} m/Pa. Temperature and pressure profiles measured in the well during injection, warm-up and discharge were evaluated; and the formation temperature, initial pressure conditions in the vicinity of the well, and the locations of possible aquifers in the well were determined. Two main and two minor feed zones are seen in the well. The formation temperature was evaluated, but the best result for the formation temperature was obtained by using the last static temperature profile measured before flow commenced in the well.

1. GENERAL DESCRIPTION OF THE THEISTAREYKIR AREA

The Theistareykir high-temperature geothermal area lies in the Theistareykir fissure swarm in NE-Iceland. The location of the study area is shown in Figure 1 and its main structural features in Figure 2. The active part of the geothermal area lies in the eastern half of the Theistareykir fissure swarm. Hydrothermal alteration is also evident on the western side of the swarm, but surface thermal activity seems to have died out there some 1000 years ago. The geothermal activity covers a 10.5 km^2 area and the most intense activity is on the northwest and northern slopes of Mt. Baejarfjall and in the pastures extending from there northwards to the western part of Mt. Ketilfjall. If the old alteration in the western part of the swarm is considered to be a part of the thermal area, its coverage is nearly 20 km^2 (Ármannsson, et al., 1986).

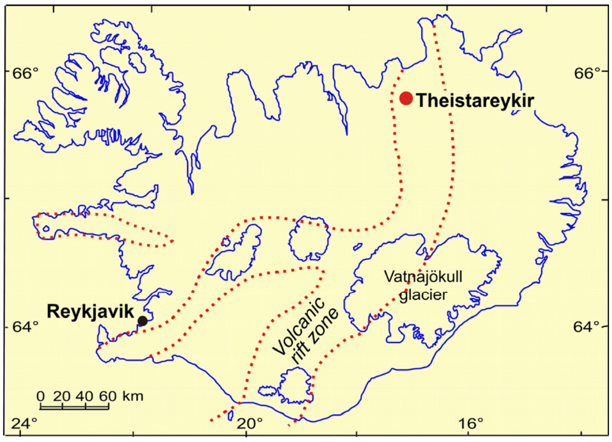

FIGURE 1: Location of the Theistareykir area

The bedrock in the area is divided into breccias (hyaloclastites) from subglacial eruptions during the Ice Age, interglacial lava flows, and recent lava flows (younger than 10,000 years), all of which are basaltic. Acid rocks are only found on the western side of the fissure swarm, from a subglacial eruption during the last glaciation or the last but one. Rifting is still active in the fissure swarm, and faults and fractures active in recent times are shown in Figure 2. One of the striking features of the fissure swarm is a bend, the reason for which is not known, but its relationship to the thermal area is evident. The north-westerly trend observed was also found in the geophysical and chemical surveys (Ármannsson et al., 1986).

Volcanic activity has been relatively infrequent in the area in recent times. Approximately fourteen volcanic eruptions have occurred in the last 10,000 years, but none during the last 2,500 years. Large earthquakes (up to M: 6.9) occur on the Tjörnes fracture zone, just north of the area, which is a right lateral transformation fault. They can also occur in the fissure swarm itself during rifting. The Tjörnes fracture zone strikes northwest, crosscutting the north-striking fractures as it enters the fissure swarm some 5 km north of the main geothermal area. The Tjörnes fracture zone remains seismically very active (Ármannsson, et al., 1986).

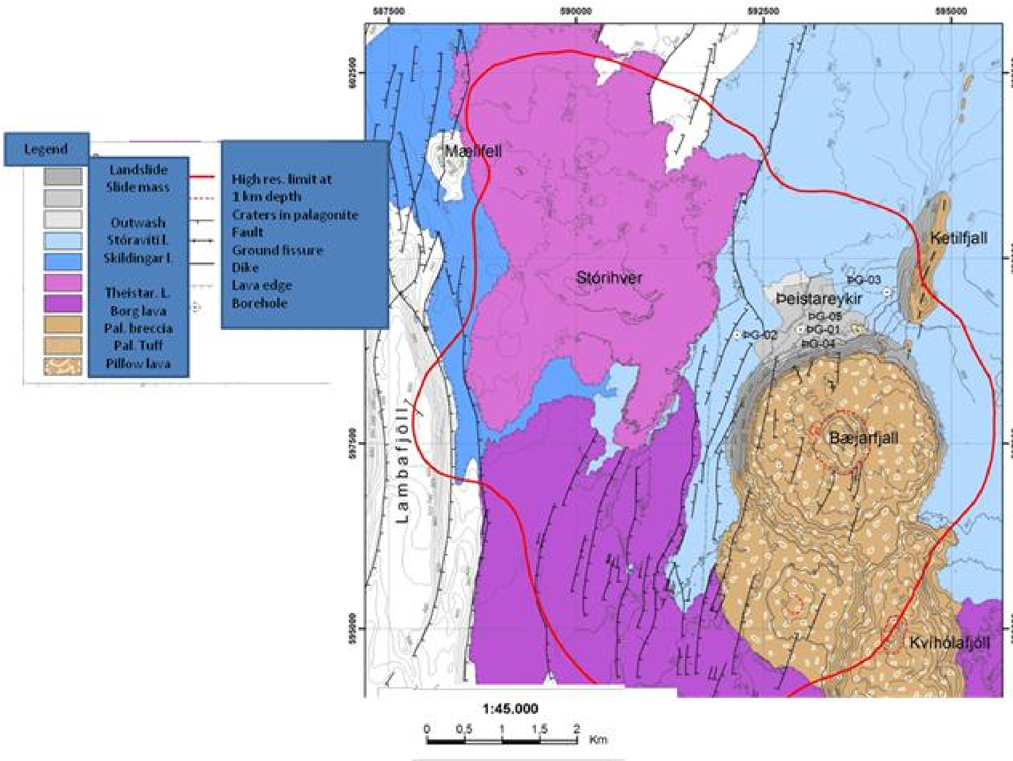

FIGURE 2: The main structural features of the Theistareykir area (Ármannsson, 2008)

2. WELL TESTING

2.1 Theoretical background

Well testing is a critical phase in the development of any geothermal resource. During a well test, the response of a reservoir to changing production or injection (q) is monitored. Since the response is, to a greater or lesser degree, characteristic of the properties of the reservoir, it is possible in many cases to infer reservoir properties from the response. Well test interpretation is, therefore, an inverse problem in which model parameters are inferred by analysing model response to given input.

In most well test cases, the reservoir response that is measured is the pressure response (p). Hence, in many cases the well test analysis is synonymous with the pressure transient analysis. Pressure transients are due to changes in production or the injection of fluids; hence, the flow rate is treated as a transient input and the pressure as a transient output (Earlougher, 1977; Horne, 1995).

2.2 Pressure diffusion equation

The three governing laws that are used in deriving the pressure diffusion equation are the following (Earlougher, 1977; Horne, 1995).

a) Law of conservation of mass

Mass flow in - Mass flow out = Rate of change of mass accumulation

b) Law of conservation of momentum, or Darcy's law (here in radial coordinates):

$$q = 2\pi h \frac{k}{\mu} \frac{\partial P}{\partial r} \tag{1}$$

where q = Volumetric flow rate per unit length (m^3/ms);
h = Reservoir thickness (m);
k = Formation permeability (m^2);
P = Reservoir pressure (Pa);
r = Radial distance (m);
μ = Dynamic viscosity of water (kg/ms).

c) Equation of state for water:

$$c = \frac{1}{p} \left(\frac{\partial \rho}{\partial P}\right)_T \tag{2}$$

where c = Compressibility of water (Pa^{-1});
ρ = Density of water (kg/m^3);
T = Temperature (°C).

From Equations 1 and 2, the following radial pressure diffusion equation can be derived:

$$\frac{\partial}{\partial r}\left(\frac{r\partial P(r,t)}{\partial r}\right) = \frac{\mu c_t}{k}\left(\frac{\partial P(r,t)}{\partial t}\right) \tag{3}$$

where $P(r,t)$ = Reservoir pressure at a distance r and time t (Pa);
c_t = Compressibility of wet reservoir formation (Pa^{-1});
t = Time (s).

The radial pressure diffusion equation is a partial differential equation that describes isothermal flow of fluid in porous media and how the pressure $P(r,t)$ diffuses through the reservoir. Initial and boundary conditions are required to solve for $P(r,t)$ (Steingrímsson, 2002). For an infinite acting reservoir, the boundary conditions are:

a) Initial conditions:

$$P\,(r,t) = P_i \text{ for } t = 0, r > 0 \tag{4}$$

where P_i = Initial reservoir pressure (Pa).

b) Inner and outer boundary conditions:

$$P\,(r,t) = P_i\, r \to 0 \quad \text{and} \quad t > 0 \tag{5}$$

$$q = 2\pi r \frac{kh}{\mu}\frac{\partial P}{\partial r} \quad r \to 0 \quad \text{and} \quad t > 0 \tag{6}$$

The solution of the radial pressure diffusion equation, *P(r,t)*, for the above initial time and boundary a condition is then:

$$P\,(r,t) = P_i + \frac{q\mu}{4\pi kh} E_i\left(-\frac{\mu c_t r^2}{4kt}\right) \tag{7}$$

E_i is the exponential integral function defined as:

$$E_i\,(-x) = -\int_x^{\varphi}\left(\frac{e^{-u}}{u}\right)du \quad \text{with} \quad x = -\frac{\mu c_t r^2}{4kt}$$

For $x < 0.01 \implies E_i\,(-x) = y + \ln x,$

where y = 0.5772 is Euler's constant.

Therefore, if $t > 100\ \mu c_t\, r^2 / 4k$ and if one uses $\ln x = 2.303 \log x$, then the solution for the radial pressure diffusion equation can be simplified to:

$$P\,(r,t) = P_i + \frac{2.303 q\mu}{4\pi kh}\left[\log\left(\frac{\mu c_t r^2}{4kt}\right) + \frac{y}{2.303}\right] \tag{8}$$

This solution for the radial pressure diffusion equation is called the Theis solution or line source solution (Hjartarson, 2002). In deriving the Theis solution, the following assumptions are inherent:

1. The flow is considered isothermal and radial;
2. The reservoir is homogenous, isotropic, has an infinite horizontal extent, and uniform thickness;
3. The production well penetrates the entire formation thickness;
4. The formation is completely saturated with a single-phase fluid.

2.3 Semi-logarithmic well test analysis

The Theis solution can be written as:

$$P\,(r,t) - P_i = \frac{2.303 q\mu}{4\pi kh}\left[\log\left(\frac{4k}{\mu c_t r^2}\right) - \frac{y}{2.303}\right] + \frac{2.303 q\mu}{4\pi kh} \tag{9}$$

The above equation is in the form: $\Delta P = A + \log t$, which is a straight line with the slope *m* on a semilog graph where:

$$\Delta P = P\,(r,t) - P_i; \quad A = \frac{2.303 q\mu}{4\pi kh}\left[\log\left(\frac{4k}{\mu c_t r^2}\right) - \frac{y}{2.303}\right], \quad \text{and} \quad m = \frac{2.303 q\mu}{4\pi kh}$$

The formation transmissivity, *T*, can be calculated from the slope of the semi-log straight line by

$$T = \frac{kh}{\mu} = \frac{2.303 q}{4\pi m} \tag{10}$$

If the temperature is known, then the dynamic viscosity, μ can be inferred from steam tables, thus, the permeability thickness, *kh*, may be calculated as follows:

$$kh = \frac{2.303q\mu}{4\pi m} \tag{11}$$

The formation storativity or storage coefficient, $S = c_t\, h$, is then obtained from the intercept with the ΔP axis when the permeability thickness is known. The Theis solution can then be written as:

$$\frac{\Delta P}{m} = \left[\left[\log\left(\frac{4kh}{\mu}\right)\left(\frac{1}{S}\right)\left(\frac{t}{r^2}\right)\right] - \frac{y}{2.303}\right] \tag{12}$$

$$\Rightarrow 10^{\frac{\Delta P}{m}} = \left(\frac{kh}{\mu}\right)\left(\frac{1}{S}\right)\left(\frac{t}{r^2}\right)\left(4 \times 10^{-\frac{\Delta P}{m}}\right) \tag{13}$$

And the storativity can be obtained as:

$$S = 2.25\left(\frac{kh}{\mu}\right)\left(\frac{t}{r^2}\right) \times 10^{-\frac{\Delta P}{m}} \tag{14}$$

Since, the transmissivity $T = kh/\mu$, then

$$S = 2.2T\left(\frac{t}{r^2}\right) \times 10^{-\frac{\Delta P}{m}} \tag{15}$$

Thus, a plot of ΔP vs. log t gives a semi-log straight line response for the infinite acting radial flow period of a well, and is referred to as a *semi-log analysis*. The semi-log analysis is based on the location and interpretation of the semi-log straight line response that represents the infinite acting radial flow behaviour of the well. However, as the wellbore has a finite volume, it becomes necessary to determine the duration of the wellbore storage effect or the time at which the semi-log straight line begins (Earlougher, 1977; Horne, 1995).

The Theis solution for the constant rate drawdown test is based on the assumption that the down-hole production rate or injection rate changes instantaneously from zero to its constant value. However, due to the wellbore storage effect, the fluid flow out of the wellhead is not always the same as the flow from the reservoir into the well. That is, if a well is suddenly opened, the wellbore pressure will drop, causing an expansion in boiling wells and water level depletion in non-boiling wells in the beginning. Similarly, if the well is suddenly shut in, the down-hole flow does not stop immediately but slowly tapers off. Several other factors can contribute to the wellbore storage effect but the above are the main factors. Therefore, it is important to find the beginning of the semi-log straight line correctly. The wellbore storage shows up as a unit slope straight line on a log-log plot ΔP vs. t. As a working rule, there are about 1½ log cycles between the end of the unit slope straight line representing wellbore storage and the start of the purely infinite acting reservoir response. This 1½ log cycle rule provides a useful method of identifying the start of the semi-log straight line. The wellbore storage coefficient C (m^3/Pa) is defined as the volume, ΔV of the fluid that the wellbore itself will produce due to a given pressure drop, ΔP, and is written as:

$$C = \frac{\Delta V}{\Delta P} \tag{16}$$

And for a well with a free fluid level, the wellbore storage coefficient is:

$$C = \frac{V_\mu}{\rho g} \tag{17}$$

where $V\mu$ = Wellbore volume per unit length (m^3/m);
ρ = Density (kg/m^3);
g = Gravitational acceleration (m/s^2)

But for a completely filled well, the fluid compression storage coefficient is given by:

$$C = c_f V_w \tag{18}$$

where C_f = Fluid compressibility (Pa^{-1});
V_w = Volume of the wellbore (m^3/m).

Pressure transmission does not take place uniformly throughout the reservoir, since it is affected by local heterogeneities. For the most part, these do not affect the pressure change within the well, except for those reservoir heterogeneities that are in the immediate vicinity of the wellbore. In particular, there is often a zone surrounding the well which is invaded by mud filtrate or cement during the drilling or the completion of the well. This zone is called the skin zone. It produces an additional pressure drop, ΔP_5 near the wellbore to the normal reservoir pressure change due to production.

$$\Delta P_5 = \frac{q\mu}{2\pi kh} \times s \tag{19}$$

where s = Skin factor (dimensionless)

If we imagine that the skin effect is due to a damaged zone of radius r_s and reduced permeability, k_s then the skin effect can be calculated from:

$$s = \left(\frac{k}{k_s} - 1\right) \ln \frac{r_s}{r_w} \tag{20}$$

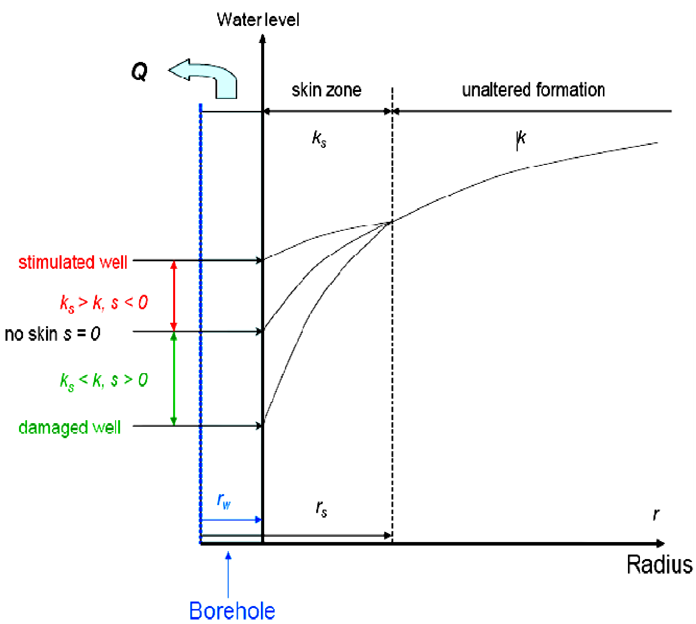

FIGURE 3: Pressure changes in the vicinity of a well due to the skin effect (Hjartarson, 2002)

We can also describe the skin effect in terms of an effective wellbore radius. This is the smaller radius that the well appears to have due to the reduction in flow caused by the skin effect. This effective radius is given by:

$$r_{weff} = r_w e^{-5} \tag{21}$$

It can be seen from Equation 20 that if the skin zone permeability k_s is higher than that of the reservoir, then the skin effect can be negative. In the case of a negative skin, the effective wellbore radius given by Equation 21 will be greater than the actual radius. The pressure distribution in this case would appear as in Figure 3.

In pumping a well with skin, the total pressure changes are given by:

$$\Delta P_t = \Delta P + \Delta P_5 \text{ or } \Delta P_t = P_i - P(r_w, t) + \Delta P_5 \tag{22}$$

or

$$\Delta P_t = \frac{-2.303 q\mu}{4\pi kh}\left[\log\left(\frac{\mu c_t r_w^2}{4kt}\right) + \frac{y}{2.303}\right] + \frac{2sq\mu}{4\pi kh} \tag{23}$$

The above equation is used to deal with the additional pressure drop due to the skin effect during well testing. In semi-log analysis, the skin factor does not affect the evaluation of transmissivity but it does affect the evaluation of storativity as shown in the following equation:

$$c_t h e^{-2s} = 2.25\left(\frac{kh}{\mu}\right)\left(\frac{t}{r_w^2}\right) \times 10^{\frac{-\Delta P}{m}} \tag{24}$$

In general, the steps involved in a semi-log analysis are:

a) Draw a log-log plot of ΔP versus Δt;
b) Determine the time at which the unit slope line representing the wellbore storage ends;
c) Note the time of 1½ cycles after that point, which is the time at which the semi-log straight line can be expected to start;
d) Draw a semi-log plot of ΔP versus Δt;
e) Look for the straight line, starting at the suggested time point;
f) Estimate the transmissivity and storativity depending on the skin effect;
g) Estimate the skin factor.

2.4 Dimensionless variables and type curve well test analysis

Well test analysis often makes use of dimensionless variables in order to simplify the reservoir models by embodying the reservoir parameters, thereby generalizing the pressure equations and solutions. They have the advantage of providing model solutions that are independent of any particular unit system. Different reservoir models may have different boundary conditions giving rise to different solutions of the pressure diffusivity equation. Some of the solutions are mathematically complicated and are, therefore, expressed as type curves that are dimensionless solutions associated with a specific reservoir model. Each appropriate reservoir model of a well test is found by plotting pressure transient data from a well test on a log-log graph and comparing it with various type curves. The following dimensionless variables are substituted in the pressure diffusion equation:

a) Dimensionless pressure, P_D

$$P_D = \frac{2\pi kh}{q\mu}\left(P_i - P(r,t)\right) \tag{25}$$

b) Dimensionless time, t_D

$$t_D = \frac{kt}{c_t \mu r^2} \tag{26}$$

c) Dimensionless radius or distance, r_D

$$r_D = \frac{r}{r_w} \tag{27}$$

Generally, the procedure for type curve analysis can be outlined as follows:

1. The data is plotted as $\log \Delta P$ vs. $\log \Delta t$ on the same scale as that of the type curve.
2. The curves are then moved, one over the other, by keeping the vertical and horizontal grid lines parallel until the best match is found.
3. The best match is chosen and the pressure and time values are read from fixed points on both graphs: ΔP_m, ΔP_{DM}, P_{DM}, Δt_M, and t_{DM}.
4. For an infinite acting system, the transmissivity, T, is evaluated from:

$$T = \frac{kh}{\mu} = \frac{q}{2\pi}\frac{P_{DM}}{\Delta P_M} \tag{28}$$

5. And the storativity, S, is calculated as:

$$S = c_t h = \frac{kh}{\mu r_w^2}\frac{\Delta t_m}{t_{DM}} \tag{29}$$

3. INJECTION TESTS

An injection test is usually performed in high-temperature wells at the end of drilling. Water is then injected into the well and the pressure response is monitored. The injection rate is changed in steps during the test, increasing or decreasing the rate in order to observe the different pressure responses in the well. From the information gathered it is possible to estimate different parameters of the well and the surrounding reservoir, such as the injectivity index, storativity, transmissivity and permeability, using the methods described in Section 2.

3.1 Testing of well THG-1

The injection test of well THG-1 at the Theistareykir geothermal area was performed on the 5th and 7th of September, 2002. The pressure gauge was located at 1,600 m which was believed to be the representative reservoir pressure depth (pivot point). At this depth, the reservoir controls the pressure in the well and, therefore, the measured response can be used to estimate not only well parameters but also reservoir parameters. The measured pressure response can be seen in Figure 4. Before the injection test started on the 5th of September, injection was constant at 20 l/s of water, to wash out the formation from invasions of filtrate and cuttings formed during drilling, and also to alleviate the skin effect problem and achieve a stabilized flow rate before the injection test. At 16:40 the injection was increased to 34.1 l/s and at 19:30 the injection was increased to 55.2 l/s. After the two first steps the injectivity index was calculated and found to be increasing between steps 1 and 2 (Figure 4). Since the calculated properties of the well were changing between the steps the decision was made to

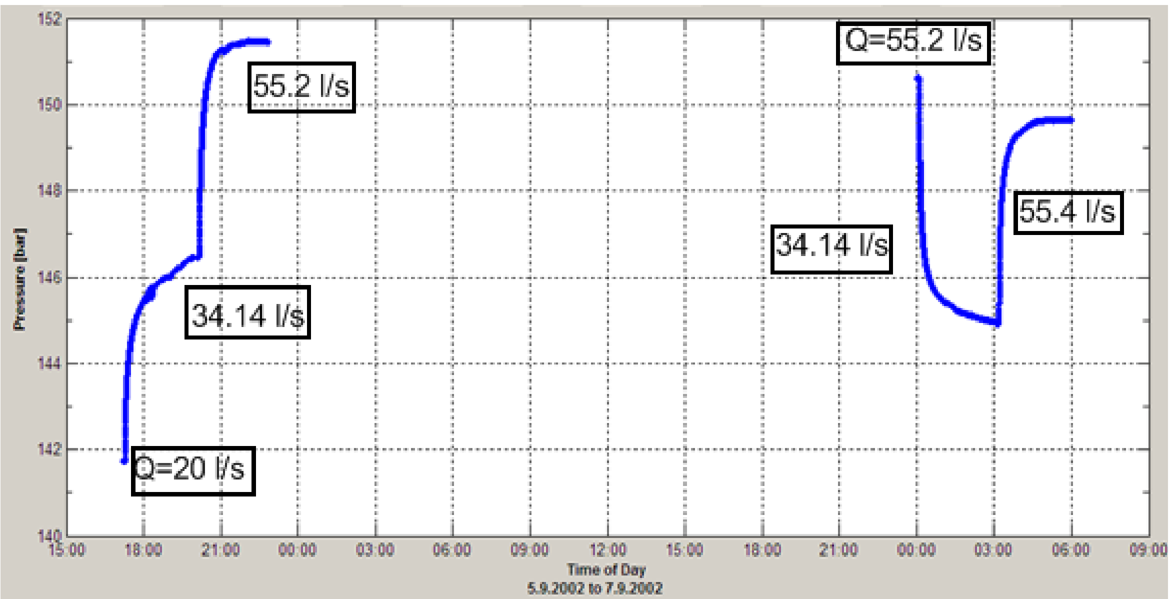

FIGURE 4: Pressure changes at 1,600 m depth in well THG-1 during injection testing

stimulate the well. After 12 hours injection was again began at the same rate as before, 55.2 l/s. At 00:00 (after 24 hours) the injection was decreased to 34.14 l/s and then increased to 55.4 l/s at 03:00. In Figure 4, it can be seen that the pressure is 1 bar lower at the beginning of step 3, after the stimulation, than at the end of step 2, before the stimulation. This indicates that the well has changed during the stimulation; fractures have opened.

To model the data (pressure vs. time) during the injection test, a software called WellTester was used (Júlíusson et al., 2007). WellTester was developed by ISOR – Iceland GeoSurvey. Figure 4 and Table 1 show that the injectivity index changes considerably between the first two steps but is similar for the last two steps. This indicates that the well's properties changed during stimulation of the well. So to get a good fit in WellTester, the data were loaded separately.

TABLE 1: Summary of the results from the non-linear regression parameter estimate using injection test data from well THG-1

	Storativity S ($m^3/(Pa \cdot m^2)$)	**Transmissivity T ($m^3/(Pa \cdot s)$)**	**Skin factor, s**	**Wellbore storage C (m^3/Pa)**	**Permeability thickness kh (Dm)**	**Injectivity index II ((l/s)/bar)**
Step 1	4.96×10^{-8}	1.44×10^{-8}	-3.20	7.96×10^{-6}	1.11	3.27
Step 2	2.94×10^{-8}	4.30×10^{-8}	-0.79	1.55×10^{-5}	3.25	4.53
Step 3	3.88×10^{-8}	4.05×10^{-8}	-0.18	1.05×10^{-5}	3.07	3.72
Step 4	3.37×10^{-8}	4.41×10^{-8}	-0.39	1.12×10^{-5}	3.34	4.37
Steps 1-2 together	1.79×10^{-8}	2.35×10^{-8}	-2.67	3.77×10^{-6}	1.77	3.90
Steps 3-4 together	1.26×10^{-7}	2.35×10^{-8}	-1.64	6.76×10^{-6}	1.79	4.04

3.2 Well test results

Assuming a reservoir temperature of 330°C the WellTester program can estimate the reservoir pressure P, wellbore radius r_w, the dynamic viscosity of reservoir fluid μ, the total compressibility c_t, and the porosity φ. All the values of those parameters are shown in Table 2.

TABLE 2: Summary of the initial parameters given in the well test

Parameter name	**Parameter value**	**Parameter unit**
Estimated reservoir temperature (test)	330	[°C]
Estimated reservoir pressure (pest)	147.50	[bar]
Wellbore radius (r_w)	0.20	[m]
Dynamic viscosity of reservoir fluid (μ)	7.57×10^{-5}	[Pa·s]
Compressibility total	1.05×10^{-9}	[1/Pa]
Porosity (φ)	0.10	[-]

With the WellTester set at 330°C and 147.5 bars, the values for the temperature and pressure were compared with the values in Figures 15 and 16, presented in Section 3.4. It can be seen that these values fit for this depth. For all steps it was assumed:

- That the reservoir is homogenous;
- That the boundary is infinite;
- That the well has a constant skin; and
- That it also has wellbore storage.

To get a good fit with the WellTester program, the data was separated into two parts: (1) Steps 1-2 before stimulation of the well and (2) steps 3-4 after stimulation of the well. Each step was also modelled separately and the parameters were calculated for each step and then compared for all steps (Table 1).

Modelling step 1:
Using the Theis model, non-linear regression analysis was performed to find the parameters that best fit the data gathered. The results from the regression analysis are shown graphically for step 1 in Figure 5. Figure 6 shows additional plots of the same data on a log-linear scale (left) and log-log scale (right). The plot on the right also shows the derivative of the pressure response, multiplied with the time passed since the beginning of the step. This trend is commonly used to determine which type of model is most applicable to the observed data. The modelled response fits quite well with the original data (Figure 5).

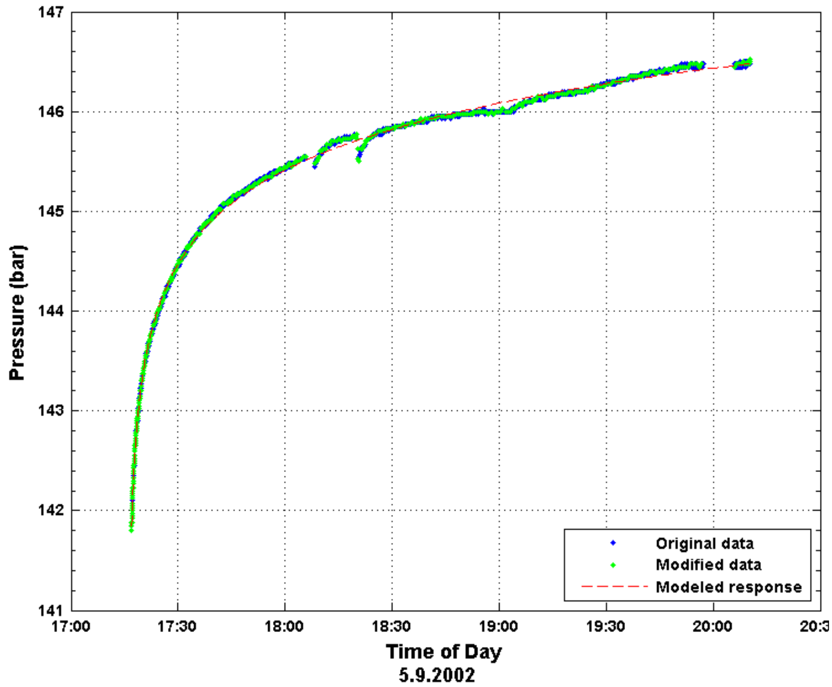

FIGURE 5: Fit between the model and the collected data for step 1 of the well test

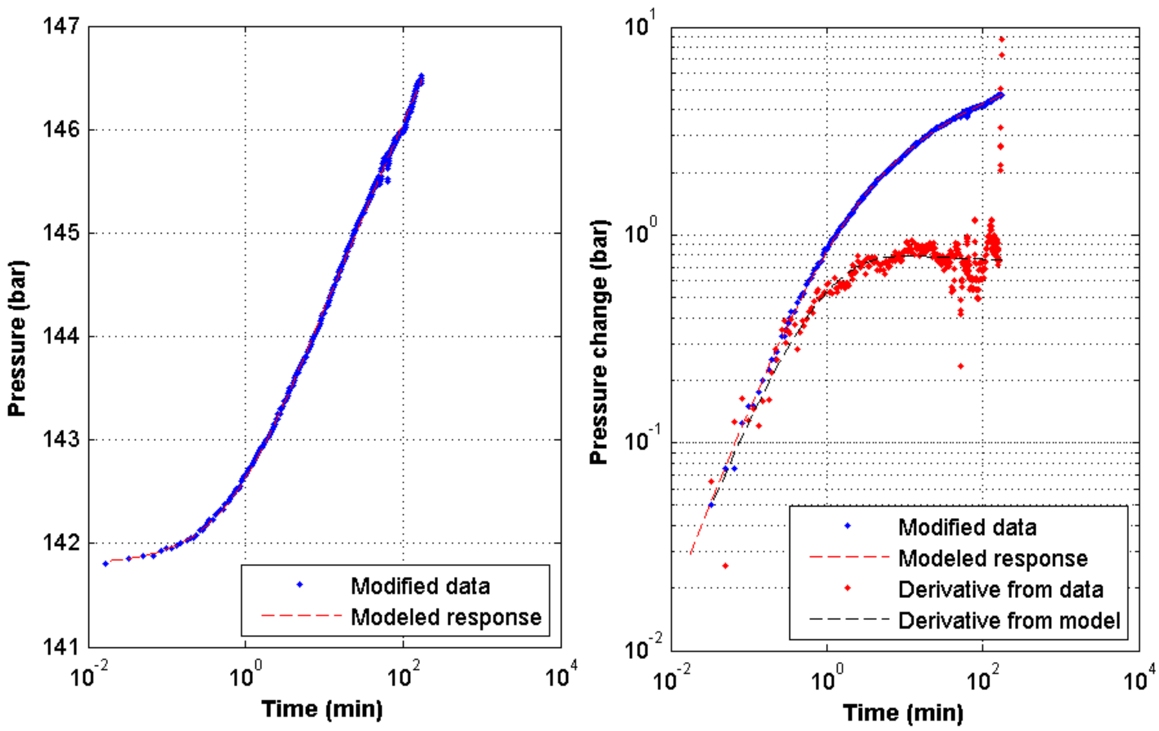

FIGURE 6 : Fit between the model and the selected data on a log-linear scale (left) and a log-log scale (right); the derivative on the right is commonly used to determine the most appropriate type of model.

Modelling step 2:
The results from the regression analysis are shown graphically for step 2 in Figure 7. Figure 8 shows additional plots of the same data on a log-linear scale (left) and a log-log scale (right). The modelled response did not quite fit the pressure response at the end of the step.

Steps 1 and 2 were modelled together and the results from the regression analysis are shown graphically in Figure 9. The model under-estimates the pressure in step 1 and overestimates the pressure in step 2. In Table 1, it can be seen that the injectivity index is 3.3 for step 1 and 4.5 for step 2.

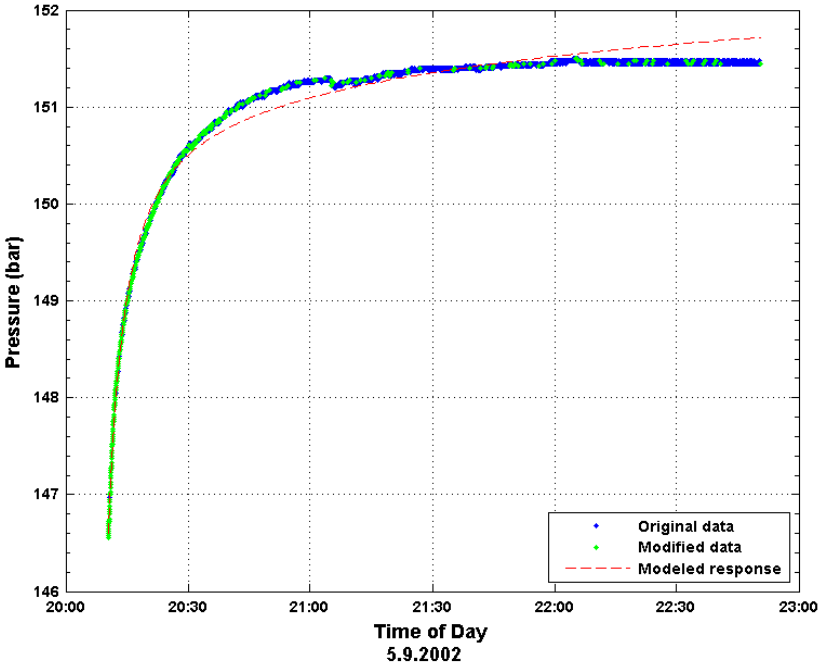

FIGURE 7: Fit between the model and the collected data for step 2 of the well test

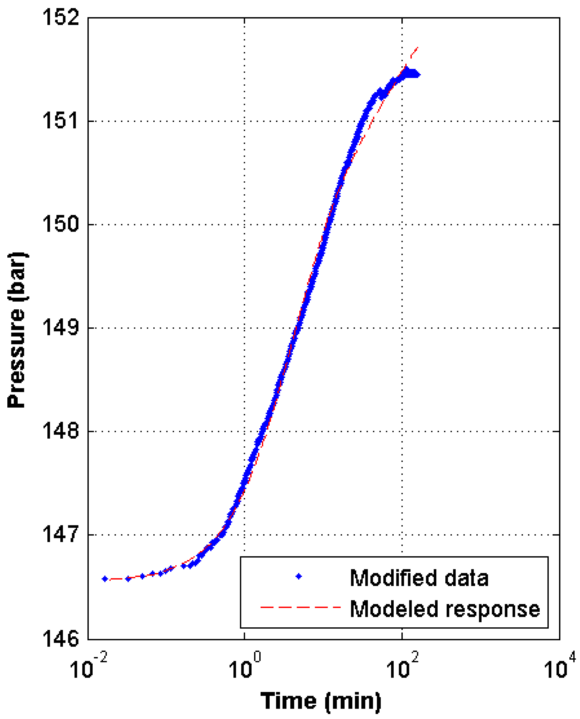

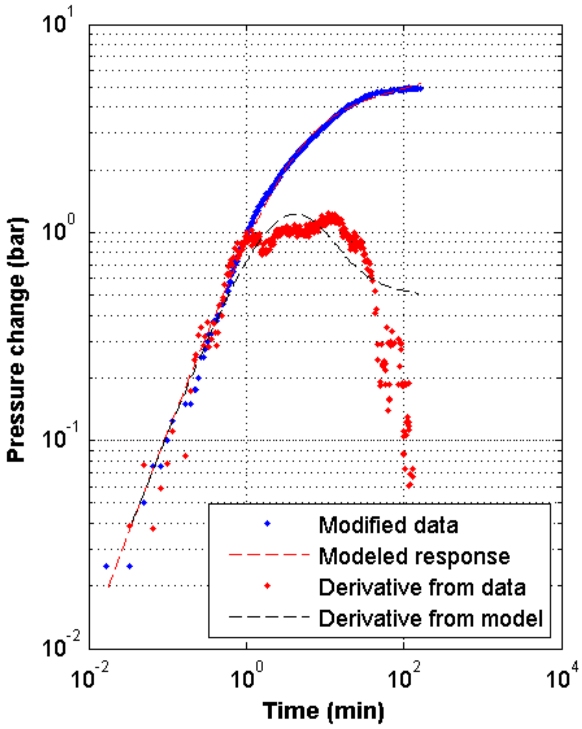

FIGURE 8: Fit between the model and the selected data on a log-linear scale (left) and a log-log scale (right)

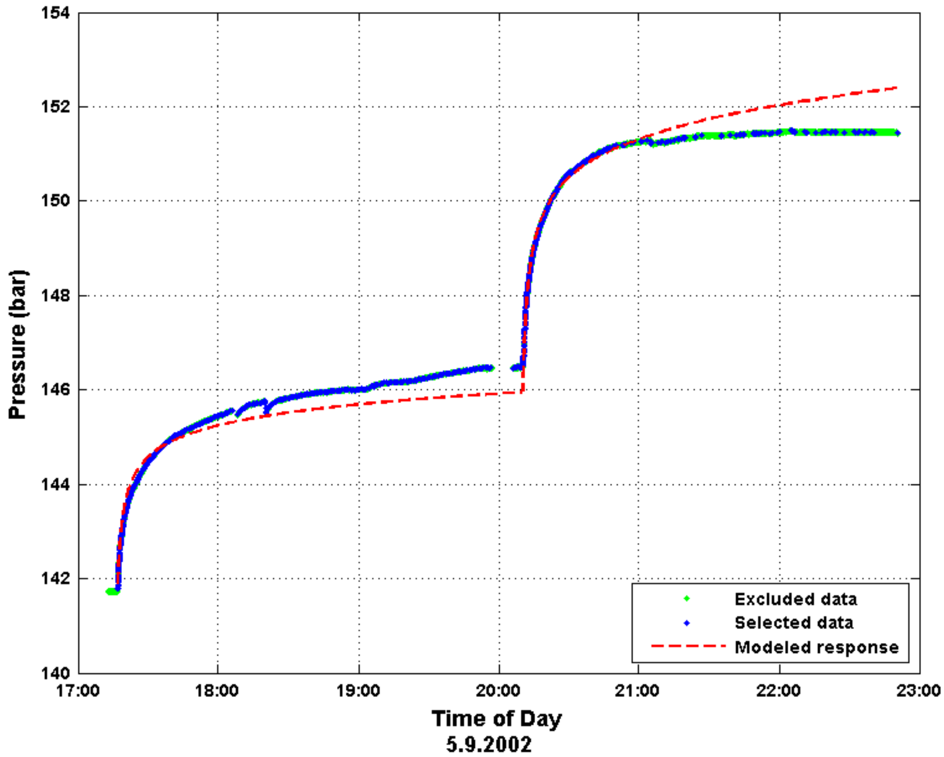

FIGURE 9: Fit between the model and the collected data for steps 1 and 2 of the well test

Modelling step 3:
The results from the regression analysis are shown graphically for step 3 in Figure 10. Figure 11 shows additional plots of the same data on a log-linear scale (left) and a log-log scale (right). The modelled response fit quite well with the original data.

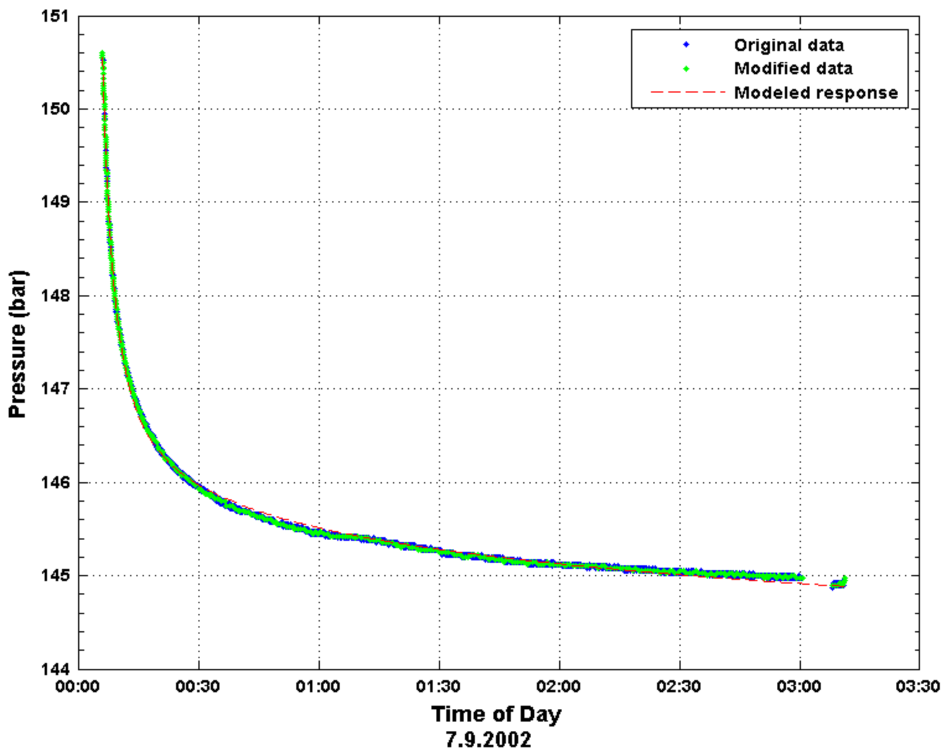

FIGURE 10: Fit between the model and the collected data for step 3 in the well test

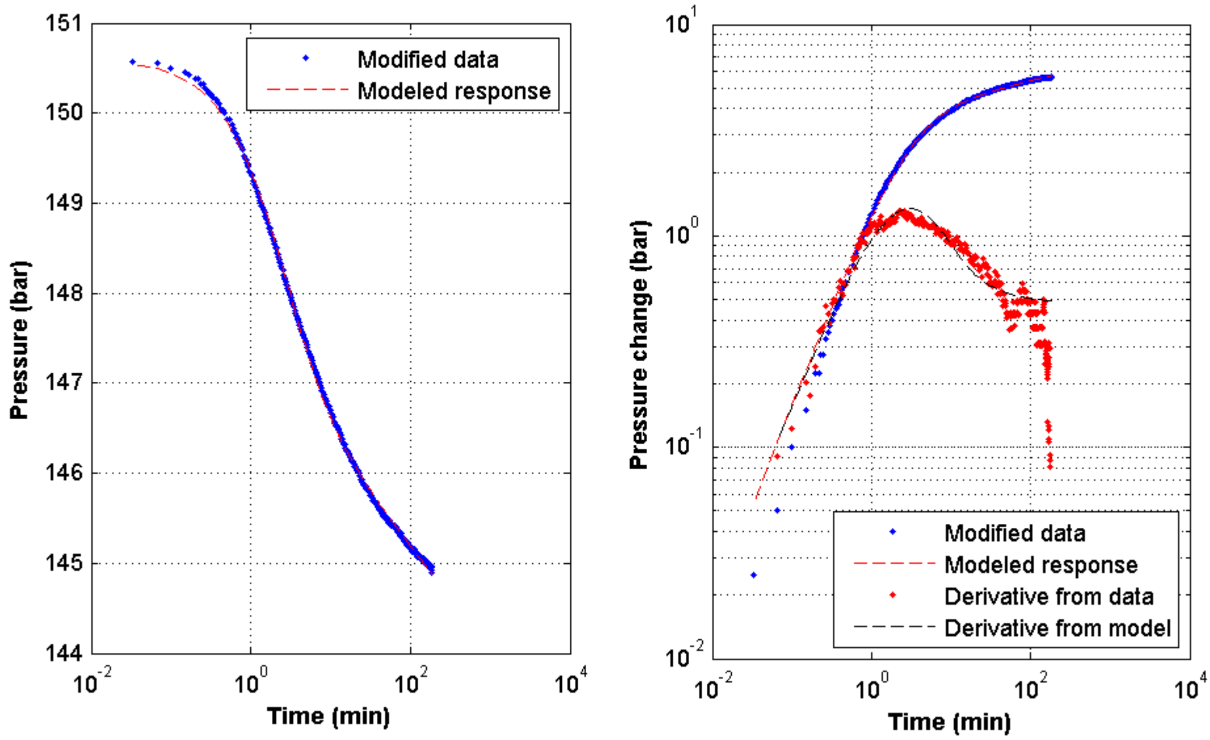

FIGURE 11: Fit between the model and the selected data on a log-linear scale (left) and a log-log scale (right)

Modelling step 4:
The results from the regression analysis are shown graphically for step 4 in Figure 12. Figure 13 shows additional plots of the same data on a log-linear scale (left) and a log-log scale (right). The modelled response fit fairly well with the original data but the same behaviour as in step 2 (Figure 5)

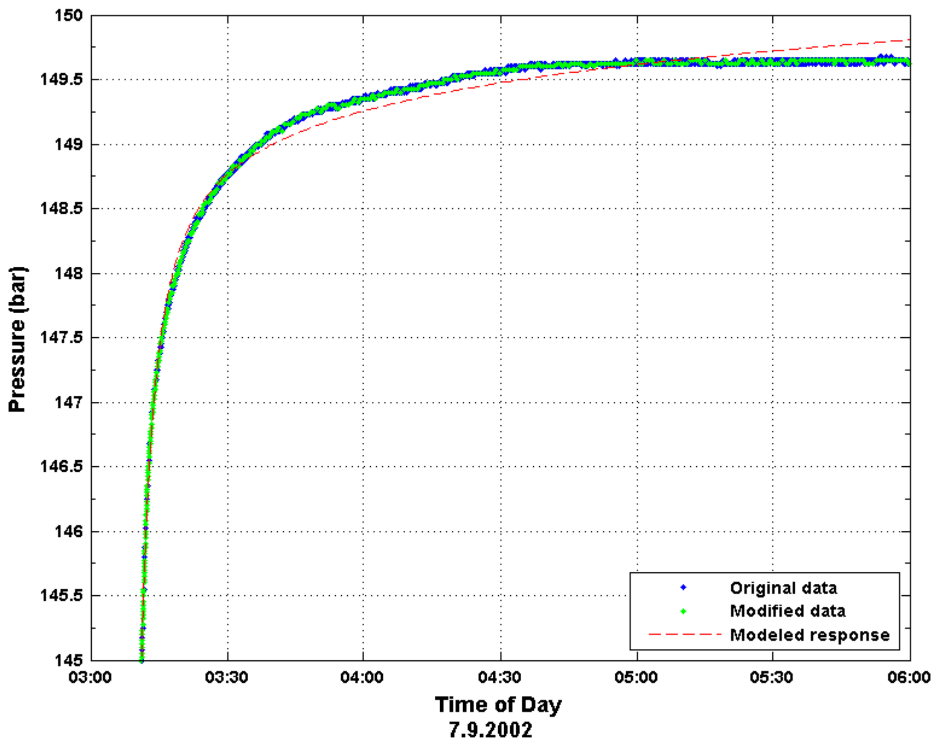

FIGURE 12: Fit between the model and the collected data for step 4 in the well test

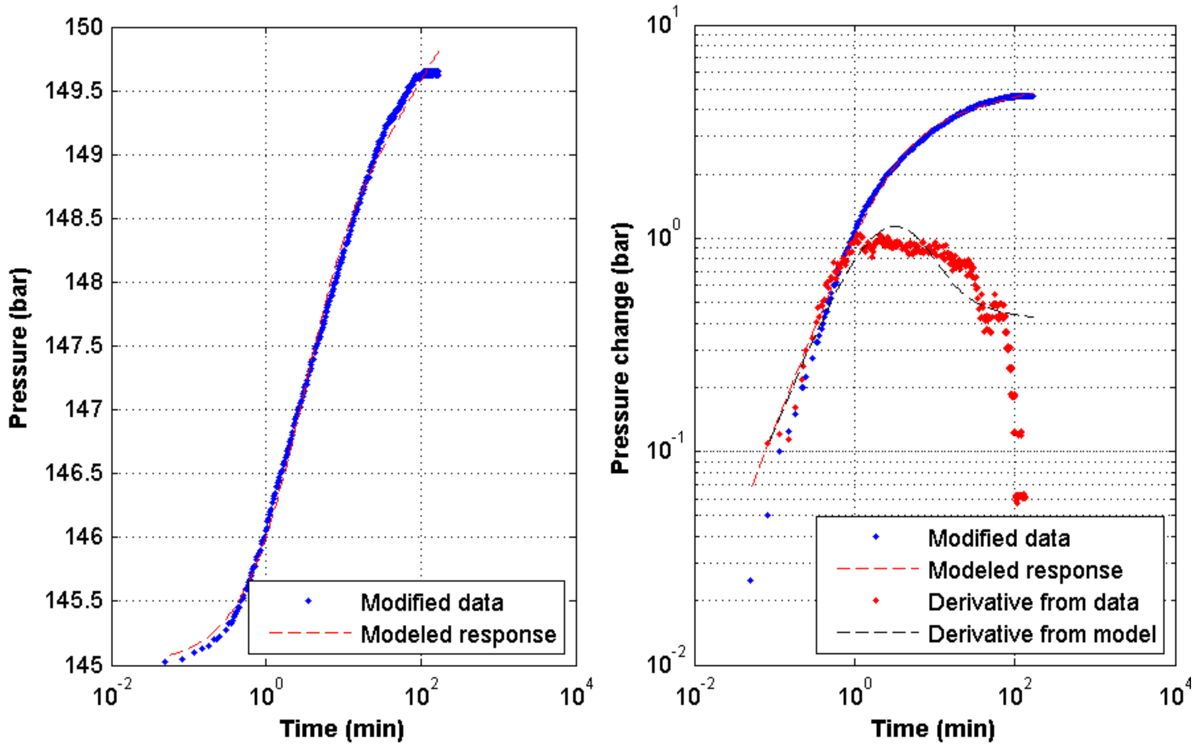

FIGURE 13: Fit between the model and the selected data on a log-linear scale (left) and a log-log scale (right)

Steps 3 and 4 were finally modelled together and the results from the regression analysis are shown graphically in Figure 14. The model overestimates the pressure change in both steps but the fit is better than for steps 1 and 2 together. In Table 1 it can be seen that the injectivity index is 3.7 for step 3 and 4.4 for step 4.

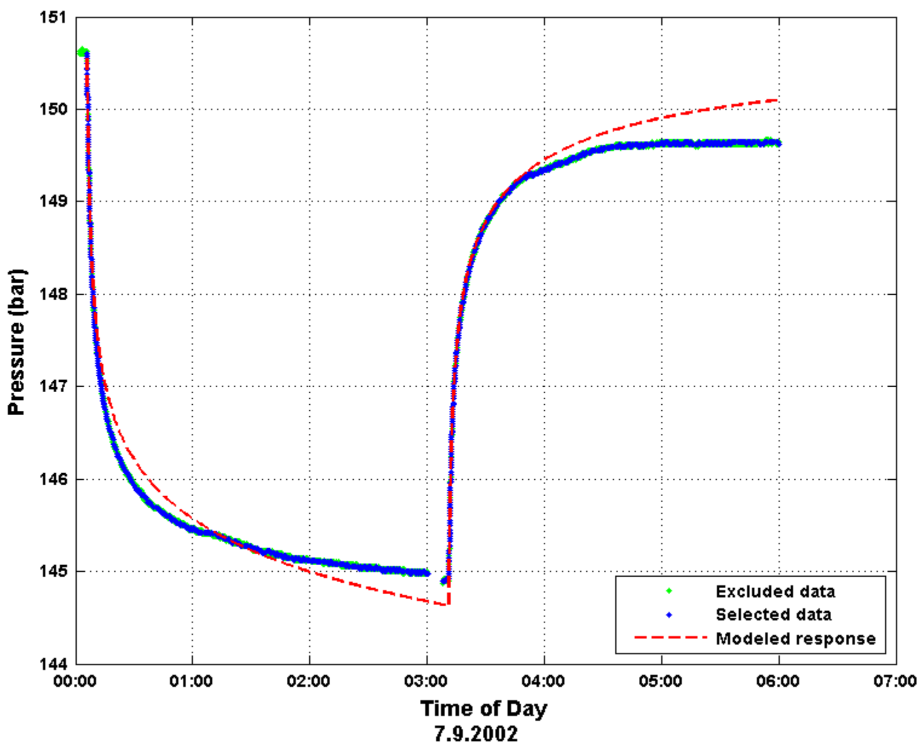

FIGURE 14: Fit between the model and the collected data for steps 3 and 4 in the well test

The WellTester software was also used to calculate the wellbore parameters for the injection steps. It enables the use of different flow models to be tried in order to fit the raw data and to calculate transmissivity, storativity, wellbore storage, and skin effects. The output plots of the WellTester program are shown in Figures 5-14 and the output parameters in Table 1. The parameters calculated for the four injection steps by the semi-log analysis are close to values generally found in Iceland.

Regarding the various other parameters of the table, it can be seen that the values found for different parameters were usually typical for the values found in Iceland. Also note that more realistic values were found when the steps where fitted separately. When all the data were added together, the values of the parameters changed drastically.

3.3 Interpretation and definition

The storativity has a great impact on how fast the pressure wave can travel within the reservoir. Also the storativity varies greatly between reservoir types (i.e. liquid-dominated vs. two-phase or dry-steam) because of its dependence on fluid compressibility (Grant et al., 1982). Common values for liquid-dominated geothermal reservoirs are around 10^{-8} $m^3/(Pa\ m^2)$ while two-phase reservoirs might have values on the order of 10^{-5} $m^3/(Pa\ m^2)$. The results for THG-1 give the storativity value of 3.37×10^{-8} $m^3/(Pa\ m^2)$. Therefore, we conclude that we have a liquid-dominated geothermal reservoir.

The transmissivity describes the ability of the reservoir to transmit fluid, hence largely affecting the pressure gradient between the well and the reservoir. The transmissivity can vary by a few orders of magnitude but common values from injection testing in Icelandic geothermal reservoirs are on the order of 10^{-8} $m^3/(Pa\ s)$. The results for THG-1 give a transmissivity value of 4.4×10^{-8} $m^3/(Pa\ s)$, or a value of the same order.

The skin factor (*s*) is a variable used to quantify the permeability of the volume immediately surrounding the well. This volume is often affected by drilling operations, being either damaged (e.g. because of drill cuttings clogging the fractures) or stimulated (e.g. due to extensive fracturing around the well). For damaged wells the skin factor is positive and for stimulated wells it is negative. The skin factor in Icelandic geothermal reservoirs is commonly around -1, although values may range from about -5 to 20. The skin factor can also be described in terms of the effective wellbore radius, i.e. the apparent radius of the wellbore caused by the skin effect. The effective radius is given by $r_{eff} = r_w e^{-5}$ where r_w is the measured wellbore radius (Horne, 1995). It should be noted that the skin factor and wellbore storage are quite strongly correlated in most well test models; hence, the relative accuracy on each parameter will be lowered when both are included. In THG-1 all the values are negative which means the well is stimulated, as can be seen in Table 1.

The wellbore storage (*C*) is a property that accounts for the difference between the wellhead flow rate, and the "sand face" flow rate (i.e. the flow into or out of the actual formation). Wellbore storage effects can be caused in several ways, but most commonly by changing the liquid level and fluid expansion. In injection testing the most dominant cause for wellbore storage is changing the liquid level. The storage effect is caused by the volume of the wellbore itself being emptied or filled. In the case of a fluid expansion, consider a drawdown test. When the well is first opened to flow, the pressure in the wellbore drops and the fluid in the wellbore expands providing the initial production volume (Horne, 1995). Typically, under single-phase liquid conditions the wellbore storage is negligible because of fluid expansion. However, in a geothermal well where the wellbore fluid changes from a single-phase liquid to two-phase steam-water, the expansion effect can be very significant.

The injectivity index (*II*) is often used as a rough estimate of the connectivity of the well to the surrounding reservoir. Here it is given in the unit [(l/s)/bar] and it is defined as the change in the injection flow rate divided by the change in the stabilized reservoir pressure:

$$II = \frac{\Delta Q}{\Delta P} \tag{30}$$

The results for THG-1 are in the range of 3.3-4.5 (l/s)/bar for steps 1-4. The results for steps 3-4 are believed to be more accurate and the mean value for *II* is 4 (l/s)/bar which is the same result as when steps 3-4 were modelled together.

Two specific parameters of interest in reservoir physics can be deduced by combining the initial parameter estimates and the well test results. The parameters estimated in the well test were the transmissivity (T) and storativity (S) and given the porosity (φ), total compressibility (c_t) and dynamic viscosity (μ) one can estimate the reservoir thickness and the effective permeability from:

$$h = \frac{S}{\varphi c_t} \quad and \quad k = \frac{T\mu}{h} \tag{31}$$

However, it should be noted that the error in these estimates is as large as the combined error in the underlying parameters so, as a general rule, the results should only be viewed as a qualitative cross check on the well test results. The result for the permeability thickness in THG-1 is *3.4 Dm*.

3.4 Temperature and pressure logs of THG-1 during injection testing

Information obtained from pressure and temperature logs during drilling and the injection tests form the basis for the first guesses in locating aquifers and flow patterns inside the well. Furthermore, the determination of the minimum reservoir temperature, and the main loss or feed-zones obtained during drilling, are useful, in addition to the temperature and pressure logs, in blow-out risk evaluation, and in determining the physical state of the reservoir. The rate of change during circulation gives some idea about the flow rate and the time for warm-up, useful for protecting instruments during logging and for safety reasons. Cooling due to circulation and cold water pumping on the wellhead can be assessed, and the bottomhole temperature determined. The main problem with downhole measurements during disturbed conditions is that temperature and pressure in the wellbore do not match those in the reservoir (Björnsson, 2002; Stefánsson and Steingrímsson, 1990).

Temperature and pressure logs were measured in THG-1 during the injection test, and after completion during the warm-up period. The data were analysed to estimate the formation temperature and pressure, location of possible aquifers, and to simulate the flow pattern of the well. The pressure profiles measured during the warm-up (Figure 15) give the first measurements of the physical state of the reservoir.

Downhole temperature profiles from THG-1 are shown in Figure 16. They include three runs during injection, profiles during the warm-up period, and profiles while the well was flowing. The profiles were used to locate the main feed zone and aquifers in the well. According to the temperature profiles in Figure 16, a few aquifers can be seen. The first one is at 600 m depth and the second at around 720 m depth, where a jump in the temperature gradient was observed during injection. According to this, the first guess about the location of the main feed zone in the well is at around 1,600 m depth. During the injection test, temperature monitoring helped in locating the minor aquifers in the well. One minor aquifer is at 200 m depth. At the bottom of the well, the temperature profiles show decreasing temperature indicating a colder aquifer there. The warm up profiles, down to 600 m, show that thermal conduction dominates the warm-up of the well. The casing blocks possible aquifers here. Below 600 m, the highest temperature in the well is around 330°C at 1,950 m depth. However, deeper in the well there is a reversal in the temperature profiles, which indicates colder water beneath the main feed zone, or that the higher temperature occurs due to a lateral flow in the area.

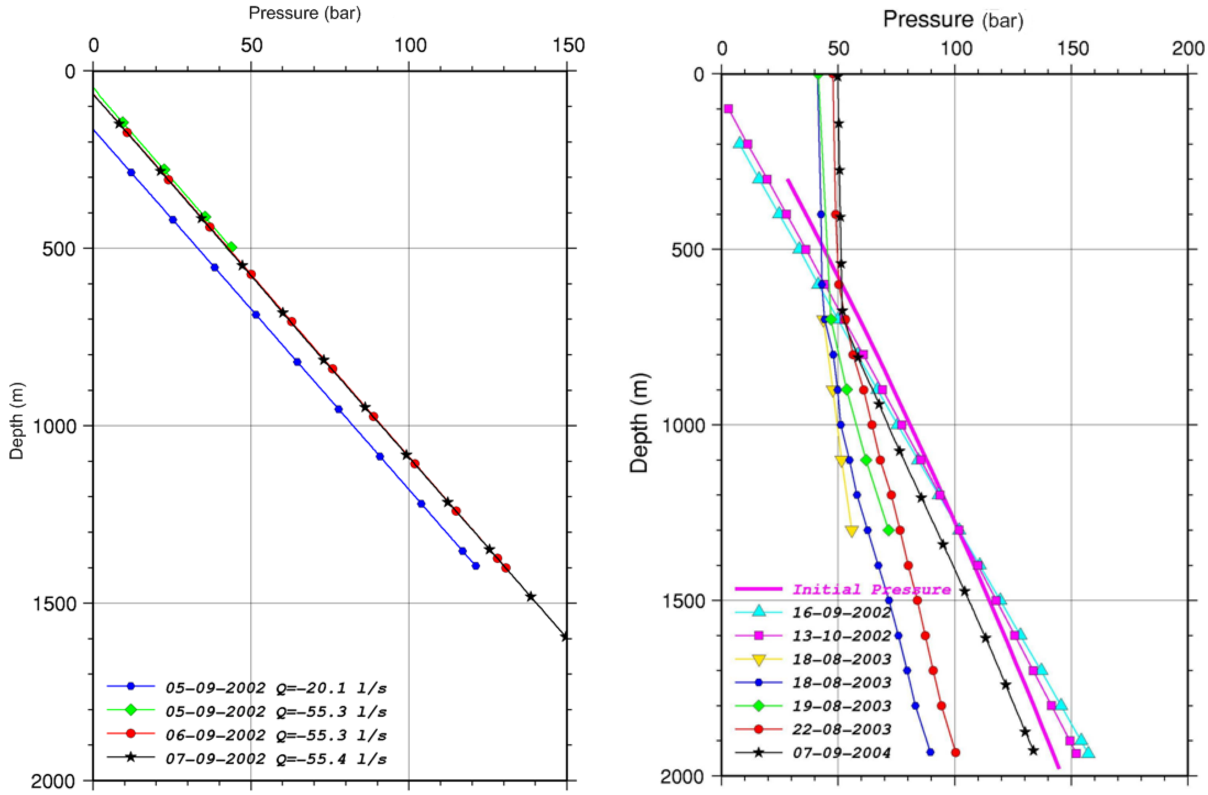

FIGURE 15: Downhole pressure during injection testing

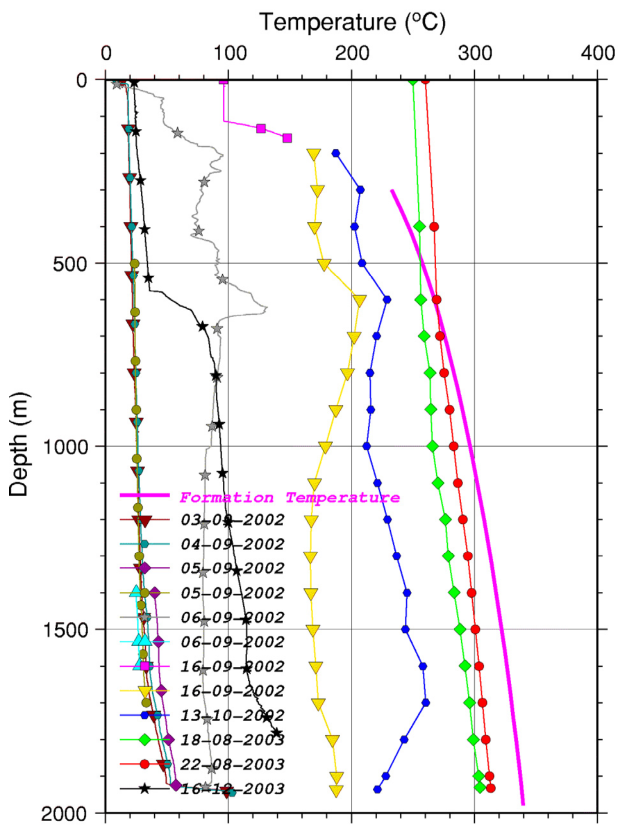

FIGURE 16: Downhole temperature during injection testing

4. LUMPED PARAMETER MODEL

Lumped parameter models have been used to simulate data on pressure changes in geothermal systems in Iceland, China, Central America, Eastern Europe and other countries (Axelsson et al., 2005). The principal purpose of the modelling is to estimate the production potential of the geothermal field and to predict the pressure response of the reservoir to different management strategies. The method handles the simulation of the pressure response of the reservoir as an inverse problem (Axelsson, 1989). This method is, therefore, not very time consuming and most importantly does not require large amounts of field data such as detailed numerical modelling of the reservoir.

4.1 Theory and methodology

A general lumped network consists of a total of N tanks with mass storage coefficients K. A tank has the mass storage coefficient K when it responds to the load of liquid mass m with the pressure $p=m/K$. The tanks are pair-wise connected by up to $N(N\text{-}1)/2$ resistors or conductors of conductivity $\sigma_{ik}(\sigma_{ii}=0)$. The mass conductivity of a resistor is σ when it transfers $q=\sigma\Delta p$ units of liquid mass per unit time at the impressed pressure differential Δp (Axelsson, 1989). The particular element σ_{ik} connects the i'th and k'th tanks and because of linearity $\sigma_{ik}=\sigma_{ki}$. The network is open in the sense that the i'th tank is connected by a resistor of conductivity σ_i to an external tank which maintains an equilibrium pressure of magnitude zero. The network is closed when $\sigma_i=0$ for i=1, 2,…N (Axelsson, 1989).

To simulate pressure response data from a liquid-dominated geothermal reservoir, an appropriate or best fitting lumped model with parameters, K and σ, is chosen. Fluid is produced from one of the tanks of the geothermal reservoir. The resulting pressure $p(t)$ is then observed in any given tank of the model (Figure 17).

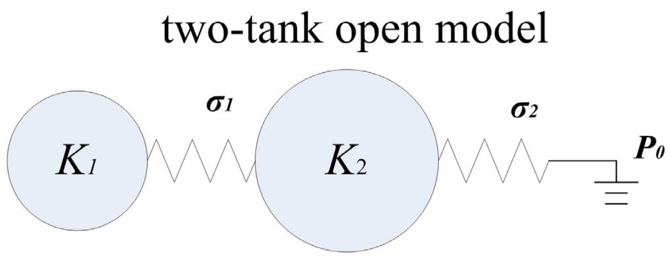

FIGURE 17: General idea of lumped parameter models

The capacity or storage in a liquid-dominated geothermal system can result from two types of capacity effects (storage mechanisms) (Axelsson, 1989). It can be controlled by:

a) Liquid/formation compressibility, such that

$$K = V\rho c_t \tag{32}$$

where V = Volume of the part of the reservoir simulated by the tank;
ρ = Liquid density;
c_t = Compressibility of the liquid-saturated formation.

The compressibility is given by:

$$c_t = \emptyset c_w + (1-\emptyset)c_r \tag{33}$$

where $\emptyset$ = Reservoir porosity;
c_w = Compressibility of the rock;
c_r = Compressibility of the rock matrix.

b) Free-surface mobility is expressed by

$$K = A\frac{\emptyset}{g} \tag{34}$$

where A = Surface area of that part of the reservoir that the tank simulates; and
g = Acceleration of gravity.

Equations 20, 30 and 31 can be used to compute the total capacity of the main area, K_1, and the recharge areas, K_2, of the geothermal system. From these values, it can be estimated that the total reservoir of the area may be due to compressibility or free surface mobility.

The geothermal model can be used to assess the production potential of the reservoir for different cases of future production. The maximum allowable drawdown in the area can be used for estimating the maximum potential of the system.

4.2 Simulation for THG-1

Lumped parameter modelling was used to simulate the pressure response during the injection test of THG-1. Because of the results from WellTester in Section 3, steps 1-2 and 3-4 were modelled separately and the results were compared to the results from WellTester. The model that best fitted the pressure data was a two-tank open model and the results can be seen in Table 3. An attempt was also made to model all steps with Lumpfit and the results can be seen in the same table.

For 1-D flow

- Confined liquid-dominated reservoir:

$$K_1 = V_1 s \tag{35}$$

$$K_2 = V_2 s \tag{36}$$

$$\sigma_1 = {}^{Ak}\!/_{Lv} \tag{37}$$

$$s = \rho_w(\emptyset c_w + (1-\emptyset)c_r) \tag{38}$$

TABLE 3: Summary of the results using the injection data with the Lumpfit model

	Step 1-2	Step 3-4	All steps
κ_1 (ms^2)	2.71282	2.71282	0.408122
κ_2 (ms^2)	109.201	109.201	136.896
σ_1 (ms)	1.72352×10^{-4}	1.72352×10^{-4}	18.2109
σ_2 (ms)	3.38979×10^{-5}	3.38979×10^{-5}	3.942
Perm. thickn. *kh* (Dm)	3.26	3.26	4.22×10^{-5}

The fit between the modelled response and the observed data in the injection test of THG-1 is seen in Figure 18 for steps 1 and 2 and in Figure 19 for steps 3 and 4. For steps 1-2 the model fits the response for the first step quite well but overestimates the response for the second step (Figure 18). This can be explained by comparing the injectivity indices for the two steps (Table 1). For steps 3-4 the modelled response fits the data much better (Figure 19). It can also be seen that the results for the injectivity index are more consistent for these two steps (Table 1).

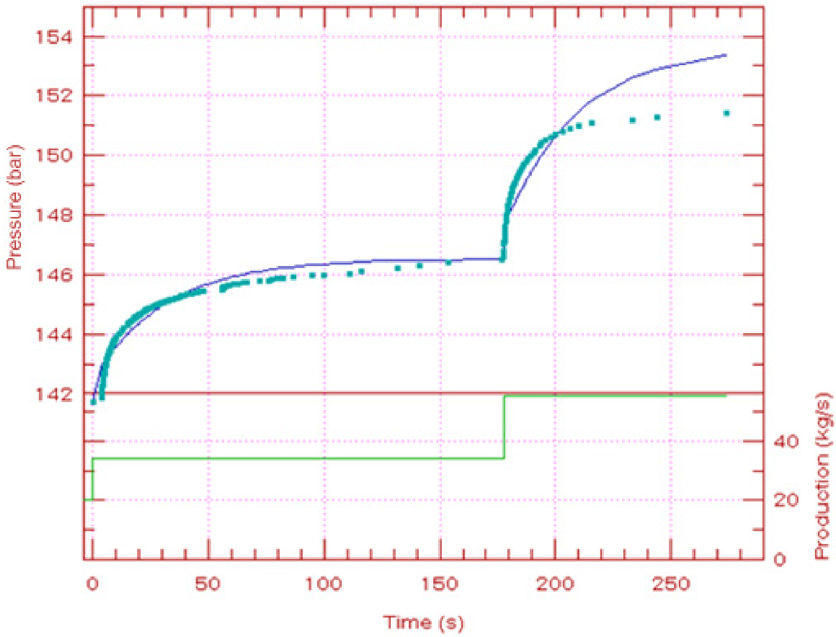

FIGURE 18: Fit between the Lumpfit model and the collected data for steps 1-2

The same parameters were used for steps 1-2 and steps 3-4 with Lumpfit (Table 3). If it is assumed that the thickness of the reservoir is 740 m, then a permeability thickness of 3.3 *Dm* is obtained. It should be remarked that when all the data was fitted together, then the models calculated the parameters differently as opposed to when it was done step by step. This problem is probably due the differences in pressure (1 bar) between the end of step 2 and the beginning of step 3, before and after the stimulation of the well (Figure 4).

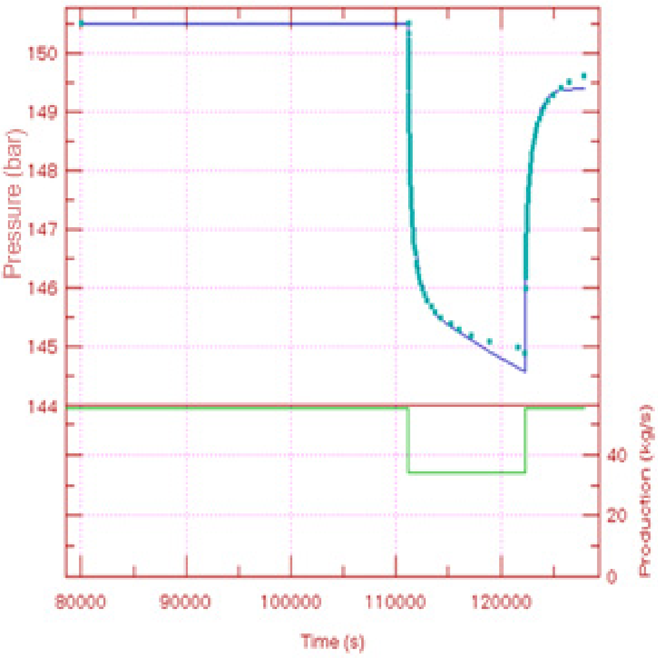

FIGURE 19: Fit between the Lumpfit model and the collected data for steps 3-4

If the results of WellTester and Lumpfit are compared, then it can be seen that the values found for the permeability thickness are similar, 3.2 *Dm* for WellTester (Table 1) and 3.3 *Dm* for Lumpfit (Table 3).

4.3 Pressure recovery

Well THG-1 at Theistareykir geothermal area was tested for production from the 22nd of October, 2002 to the 18th of August, 2003. The well was opened on the 22nd of October and the wellhead pressure (P_0), the critical lip pressure (P_c) and the flow rate of the water were measured. The total flow rate of water and steam, which is shown in Table 4, was calculated from these values (Egilsson et al., 2004). The well was in production until August, 2003 and the wellhead pressure (P_0), the critical lip pressure (P_c) and the flow rate of the water were measured a few times during this period. The total flow of water and steam during the production test of THG-1 can be seen in Table 4. The well was closed on the 18th of August and the pressure response was measured at 1,300 m depth (Figures 20 and 21).

Lumped parameter modelling was used to simulate the pressure response during the injection test of THG-1. The model that best fitted the pressure data is the two-tank open model and the results can be seen in Table 3. The fit between the modelled response and the measured data during the injection test

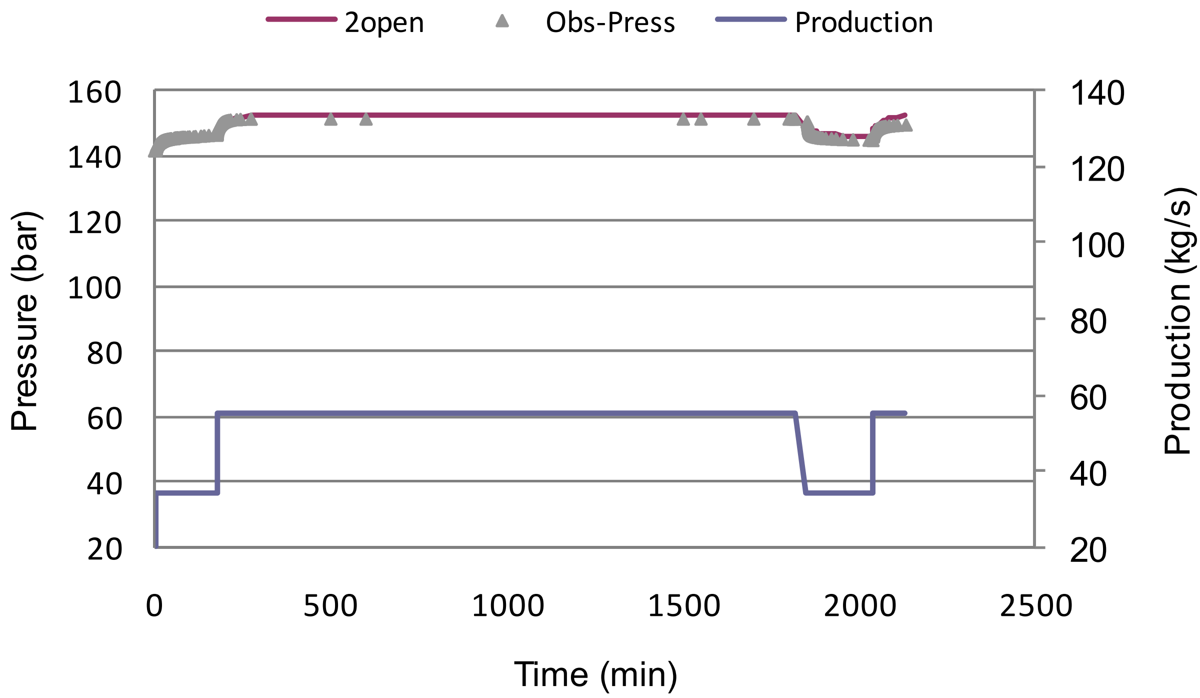

FIGURE 20: Fit between the model and the measured data during injection test

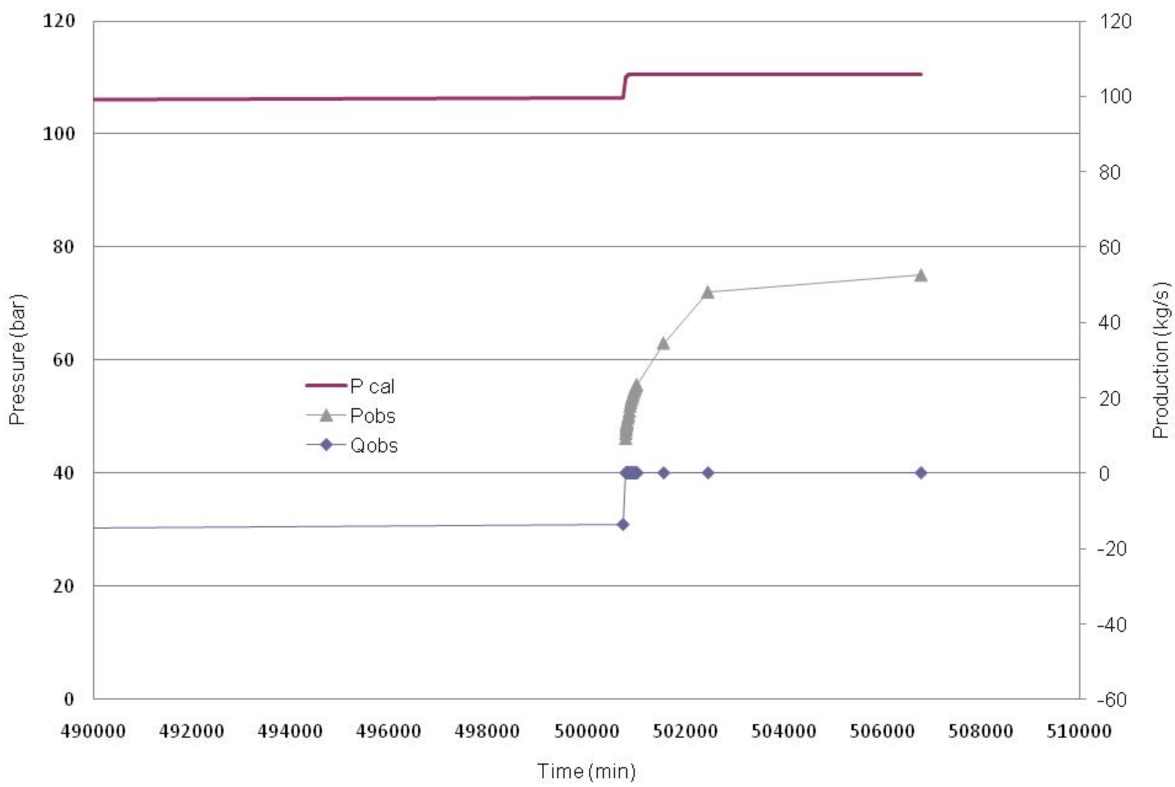

FIGURE 21: Fit between the model and the collected data for steps 3-4

is shown in Figure 20. This model was used to predict the pressure recovery of well THG-1 after the production test of 2002-2003. The production history that was used consists of the injection data during the injection test in September, 2002 and the production data during the production test from October, 2002 to August, 2003. Since the model was calibrated with pressure data during the injection test measured at 1,600 m, the prediction for the pressure will also be for the pressure at 1,600 m depth. However, the observed pressure recovery data were measured at 1,300 m depth. In order to compare the observed and calculated pressures, the calculated pressure was corrected due to the differences in hydrostatic pressure. The pressure correction was found using pressure logs from the well during the warm-up period in September and October, 2002 (Figure 15b). The calculated pressure response of well THG-1 for the production shown in Table 4 is shown in Figure 21. The measured pressure recovery at 1,300 m depth is also shown in the figure.

Note that there is a difference of about 50 bar between the pressure recovery and the pressure calculated with the two-tank open model (the best model found). Also, the pressure had not recovered to the estimated initial pressure at this depth (Figure 15b) four days after the well was closed and the last recovery measurement. With that accounted for the pressure difference is still in the range of 30-40 bar. In light of this, it is to be deduced that the model, calibrated with production data collected during injection test, is not suitable for predicting the pressure response of the reservoir due to production. A new model that takes into account all of the data from the pressure recovery would improve the prediction.

TABLE 4: Measurements of the wellhead pressure, the critical pressure and the calculated total flow rate for well THG-1 during the production test 2002-2003 (Egilsson et al., 2004)

Dates	P_0 **(wellhead pressure) (bar)**	P_c **(critical pressure) (bar)**	**Qt (total flowrate) (kg/s)**
22-10-2002 16:27	9	3	54.5
22-10-2002 16:35	7.8	2.6	44.4
22-10-2002 16:45	8.2	2.8	45.2
22-10-2002 16:55	8.5	2.8	46.8
22-10-2002 17:20	8	2.4	43.5
22-10-2002 17:40	7.9	2.3	41.5
22-10-2002 17:50	7.6	2.2	41.1
25-10-2002 12:00	7.5	2.1	29
28-10-2002 12:00	7.5	2.3	21.7
28-10-2002 12:00	12.8	2.1	26.9
2-11-2002 12:00	11.8	2.05	17.6
5-11-2002 12:00	11.7	2.18	17.9
4-12-2002 12:00	11.4	2.16	15.4
22-12-2002 12:00	11.7	2.2	15.8
5-1-2003 12:00	11.6	2.12	15.5
10-1-2003 12:00	11.3	2.16	15.6
8-2-2003 12:00	11.7	2.2	16.1
14-2-2003 12:00	11.7	2.12	16
28-2-2003 12:00	11.6	2.1	15.6
21-4-2003 12:00	11.5	2.08	15.8
1-6-2003 12:00	11.4	2.08	15.8
10-7-2003 12:00	11.4	2.07	16.2
28-7-2003 12:00	11.4	2.07	16.2
18-8-2003 12:00	28	1.45	13.7

5. CONCLUSIONS

- On making simulations with the WellTester program the results conformed to the results generally found in Iceland.
- Repeating this with the same model that the Lumpfit program gives, makes it possible to conclude that the parameters of the WellTester and Lumpfit models are nearly the same.
- The values found for the permeability thickness are similar, 3.2 Dm for WellTester and 3.3 Dm for Lumpfit.
- The Lumpfit model calibrated with short production history, data collected during injection test, is not suitable for predicting the long term pressure response of the reservoir due to production.

ACKNOWLEDGEMENTS

I would like to say 'thank you' to the Director General of CERD, Mr. Jalludin Mohamed for granting me the opportunity to attend this training. I am also grateful to Dr. Ingvar B. Fridleifsson director of the UNU Geothermal Training Programme for offering me the chance to participate in this training, and to Mr. Lúdvík S. Georgsson, deputy director, for his successful organization of the programme. Many thanks go to Ms. Saeunn Halldórsdóttir and Mr. Hédinn Björnsson, my supervisors, for their good guidance and the sharing of their knowledge and experience and supervision of this work. Sincere thanks to Ms. Thórhildur Ísberg, Mrs. Dorthe Holm, Mr. Markús A.G. Wilde, and Rósa S. Jónsdóttir for their useful help and care all through the training period.

I thank my parents for their constant prayers, support, and encouragement during the entire training period. My special thanks go to my mother for her advice and encouragement. This work is dedicated to my family, with unconditional love. May God bless them. Thanks to all the UNU fellows for their friendship and support, especially my compatriot and friend Daher Elmi Houssein. And lastly, I thank my God.

REFERENCES

Ármannsson H., 2008: The Theistareykir geothermal system, northeast Iceland. Case history. In: Georgsson, L.S., Holm, D.H., Simiyu, S.M., and Maariita, N. (eds.), *Short course III on exploration for geothermal resources.* UNU-GTP, KenGen, held in Naivasha, Kenya, CD SC-07, 10 pp.

Ármannsson, H., Gíslason, G., and Torfason, H., 1986: Surface exploration of the Theistareykir high-temperature geothermal area with special reference to the application of geochemical methods. *Applied Geochemistry, 1,* 47-64.

Axelsson. G., 1989: Simulation of pressure response data from geothermal reservoir by lumped parameter models. *Proceedings of the 14th Workshop on Geothermal Reservoir Engineering, Stanford University, California,* 257-263.

Axelsson, A., Björnsson, G., and Quijano, J.E., 2005: Reliability of lumped parameter modelling of pressure changes in geothermal reservoir. *Proceedings of the World Geothermal Congress 2005, Antalya, Turkey*, CD, 8 pp.

Björnsson, G., 2002: *Using temperature and pressure logs to determine reservoir conditions and well status*. UNU-GTP, Iceland, unpublished lecture notes.

Grant, M.A., Donaldson, I.G., and Bixley, P.F., 1982: *Geothermal reservoir engineering*. Academic Press, New York, 369 pp.

Earlougher, R.C., 1977: *Advances in well test analysis*. Soc. Petr. Eng., Monograph 5, 264 pp.

Egilson, Th., Ármannsson, H., Steingrímsson, B., Gudmundsson, Á., and Hjartarson, H., 2004: Theistareykir – well THG-1: Measurements during warm-up and production test 2002–2003. ÍSOR – Icelandic GeoSurvey, report ISOR-2004/040 (in Icelandic), 30 pp.

Horne, R.N., 1995: *Modern well test analysis, a computer aided approach* (2nd edition). Petroway Inc., USA, 65-77.

Hjartarson, A., 2002: *Pressure transient analysis (well testing theory)*. UNU-GTP, Iceland, unpublished lecture notes.
Júlíusson, E., Grétarsson, G., and Jónsson, P., 2007: *Well Tester 1.0b, user´s guide.* Iceland GeoSurvey – ÍSOR, report 2008/063, 26 pp.

Stefánsson, V., and Steingrímsson, B.S., 1980: *Geothermal logging I, an introduction to techniques and interpretation.* Orkustofnun, Reykjavík, report OS-80017/JHD-09, 117 pp.

Steingrímsson, B., 2002: *Discharge measurements and injection tests*. UNU-GTP, Iceland, unpublished lecture notes.